Mem. S.A.It. Vol. 74, 909

Memorie della

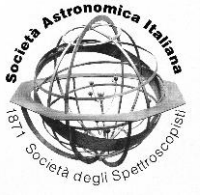

The Carina Project: Photometric Accuracy

M. Monelli[1], A.R. Walker[2], G. Bono[3], E. Brocato[7], R. Buonanno[1,3], F. Caputo[3], M. Castellani[3], V. Castellani[3,4], C.E. Corsi[3], M. Dall'Ora[1,3], M. Marconi[5], L. Pulone[3], V. Ripepi[5], M. Nonino[6], H. A. Smith[8], P.B. Stetson[9], M. Zoccali[10,]

[1] Dipartimento di Fisica, Universitá di Roma Tor Vergata, via della Ricerca Scientifica 1, Roma e-mail: monelli@mporzio.astro.it
[2] Cerro Tololo Inter-American Observatory, National Optical Astronomy Observatories, Casilla 603, La Serena, Chile
[3] INAF - Osservatorio Astronomico di Roma, via Frascati 33 00040 Monte Porzio Catone, Rome, Italy
[4] Dipartimento di Fisica, Universitá di Pisa, Piazza Torricelli 2, 56126 Pisa, Italy
[5] INAF, Osservatorio Astronomico di Capodimonte, via Moiariello 16, 80131 Napoli, Italy
[6] INAF, Sezione di Trieste, via Tiepolo 11, 34131 Trieste, Italy
[7] INAF, Sezione di Teramo, via Mentore Maggini, 64100 Teramo, Italy
[8] Dept. of Physics, Michigan State University, East Lansing, MI 48824, USA
[9] Dominion Astrophysical Observatory, Herzberg Institute of Astrophysics, NRC, 5071 West Saanich Road, Victoria, BC V9E 2E7, Canada
[10] ESO, Karl Schwarzschild Strasse 2, 85748 Garching bei Munchen, Germany

Abstract. We present B,V photometric data of the Carina dwarf Spheroidal (dSph) galaxy, collected with the Mosaic Camera ($36 \times 36 arcmin^2$) available at the 4m CTIO Blanco telescope. We discuss different reduction strategies and in particular the PSF extraction and internal accuracy reached by our measurements. We discuss a new deep Color-Magnitude Diagram (CMD) of the Carina galaxy. Finally, we show the samples of RR Lyrae, Anomalous Cepheids, and δ Scuti candidates we have detected.

Key words. Galaxies: dwarf – Galaxies: individual (Carina) – Local Group – Stars: evolution – Stars: imaging

1. Introduction

The role of dwarf galaxies is of primary interest in modern astrophysics. They are the most common objects in the present-day Universe and appear to play a key role in the formation and evolution of galaxies. Cold Dark Matter (CDM) theory suggests that they are the building blocks necessary to accrete onto bigger structures. According to this model, dSph galaxies should not have experienced any star formation event during the last few Gyrs.

Send offprint requests to: M. Monelli
Correspondence to: M. Monelli, via Frascati 33, 00040 Monteporzio Catone, Roma, Italy

On the other hand, the Local Group (LG) hosts nine dSph galaxies and these stellar systems are crucial to constrain the plausibility of this model. Although, the low surface brightness and the low central density have hampered for many years a complete census of the stellar content on these loose galaxies. In the last few years the development of wide field ($\simeq 30 \times 30'$) CCD cameras provided a good sampling of their stellar content well beyond their core radius. The new data disclosed a new interesting empirical evidence: the SFHs can vary significantly amongst LG galaxies. Moreover, the SFH of some dSphs appear very complex and characterized by bursting episodes, even in recent epochs. This evidence is at odds with theoretical predictions and further strengthens the key cosmological role of stellar populations in dSph galaxies.

Carina in this context is a very interesting target. The study of its complex star formation history disclosed the occurrence of an old ($\simeq 10Gyr$) and of an intermediate-age ($4-7Gyr$) population (Smecker-Hane et al. 1994) as well as a sizable sample of variable stars (RRLyrae, Saha et al. (1986)), Anomalous Cepheids (Dall'Ora M. et al. 2003) and dwarf Cepheids (Mateo 1998). We started a long-term project on the Carina Dwarf Spheroidal galaxy based on wide field imagers available at the 2.2 ESO/MPI and at 4m CTIO Blanco telescopes: the main target is a comprehensive investigation of static and variable stars in this galaxy.

2. Observation and Data Reduction

In the following we review the main results obtained from the data collected with the 4m CTIO telescope over three non-consecutive nights (Dec 1999 - Jan 2000) under good seeing conditions ($\leq 1arcsec$). The observing strategy was optimized to the detection of short period variable stars (from RR Lyrae down to the Turn-Off region) and 54 (B+V) phase points were secured. The total exposure time is $13,200s$ and $21,000s$ in the V and in the B-band respectively. Standard IRAF NOAO *mscred* Valdes (1997) tasks have been applied for bias subtraction and flat fielding correction. The photometry was performed with the DAOPHOTII/ALLFRAME reduction package (Stetson 1995). The magnitude of stellar-like objects is estimated with a PSF-fitting algorithm: this means that the key point of this approach is to properly model the PSF of each image. This can be done by selecting a set of bright and isolated stars. To cope with this selection we developed an automatic procedure that pins point a sample of $\simeq 150$ PSF-stars per frame to estimate the shape of the PSF. The procedure starts with an initial list of a few hundred stars, extracts a first rough PSF and then performs the fit over the entire sample of stars detected in each image. Subsequently a new list of PSF-stars is created and iteratively cleaned up according to the assumed magnitude range, photometric error, and statistical parameters. A crucial feature we have to cope in this procedure is the large field of view covered by individual chips. Individual chips are 2Kx4K pixels CCD and approximately cover an area of 18×9 arcmin. As a consequence, geometrical distortions affect the shape of the stars located in different regions of the CCD camera, and in turn the photometry might be affected by systematic positional errors. To overcome this problem the PSF-stars were selected in such a way that they uniformly sample the entire field of view of each chip.

Absolute and relative calibrations were performed by cross-correlating the final catalogue with the list of stars obtained with the 2.2m dataset (see Castellani M. et al. 2003 in these proceedings). These data have been independently calibrated (see Monelli et al. 2003), therefore we selected a large sample of secondary standard stars with colors ranging from blue HB stars to red field dwarf stars. Fig.1 shows the $(V, B-V)$ CMD for $\simeq 67,000$ stars. The mosaic displays the individual CMD obtained from each chip. The bot-

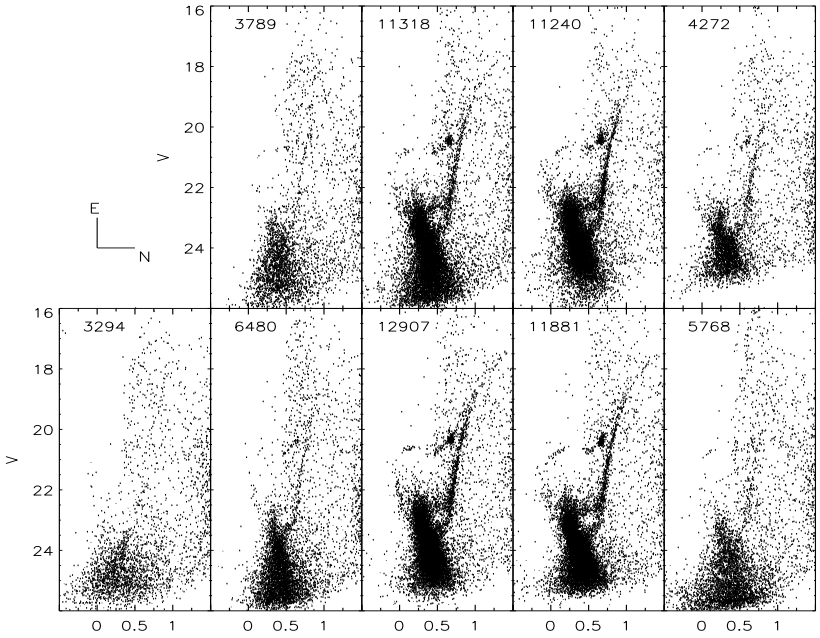

Fig. 1. CMD of the Carina central region based on B,V data collected with the 4m CTIO telescope. The photometry over $\simeq 67,000$ stars was performed with ALLFRAME. The plotted sample was selected according to the *sharpness* parameter ($|sharp| \leq 0.8$).

tom left panel is present as a consequence of the dithering that was applied during the observations. After the first night the top left chip was damaged, and therefore during the following two nights a shift of $\simeq 9'$ (one chip) was applied in the $N - S$ direction. The most external CMD discloses an interesting feature. The Carina stars are still clearly present, although this field is located at $r \simeq 25'$ from the centre of the galaxy. This means that at a distance of roughly $3R\_c$ (core radius, $\simeq 8.8'$ Mateo 1998) and relatively close to the R_t (tidal radius, $\simeq 29'$) Carina stars are still clearly present. The occurrence of extra-tidal stars has already been discussed by Kuhn et al. (1996) and more recently by Majewski et al. (2001), and according to current theoretical predictions they might be evidence of a tidal interaction with the Galaxy.

3. Clues concerning data reduction

To investigate the impact that data reduction has on the intrinsic photometric accuracy and on the limiting magnitude we decided to adopt different reduction strategies. To avoid thorny problems concerning the relative calibrations of individual chips the tests were performed using only one chip of the Mosaic Camera. The PSF-fitting photometry of V-band images was performed using two different softwares, namely ALLSTAR and ALLFRAME (Stetson 1995). The main difference between the two packages is that ALLFRAME simultaneously reduces the entire sample of (B,V) images, while ALLSTAR has to be executed over individual frames (Stetson 1995). The top panel of Fig.2 displays the V-band photometric errors obtained using the two quoted codes as a function of the mean apparent V magnitudes. Data plotted in this panel clearly show that data reduction performed with

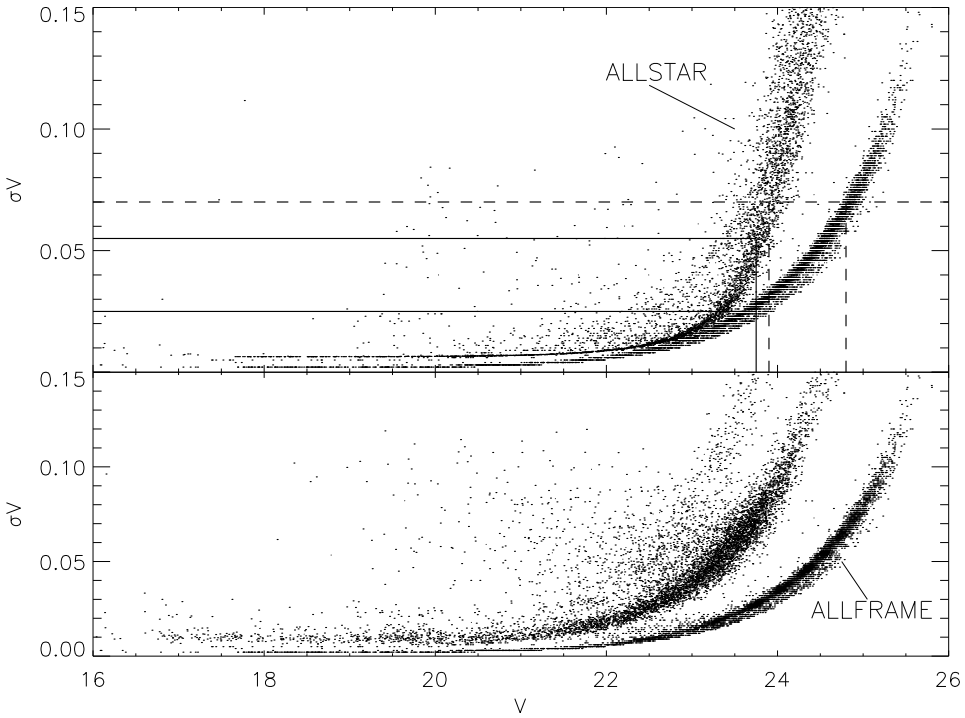

Fig. 2. Top panel: Intrinsic V-band photometric accuracy as a function of the mean magnitude. The two sets of dots refer to different data reduction strategies of the 26 V-band images. The narrow sequence on the right side displays the intrinsic accuracy of the photometry performed simultaneously running ALLFRAME over the entire data set, while the broader sequence to the photometry performed using ALLSTAR over individual V-band images. In the latter case the mean magnitudes and the relative errors are averaged *a posteriori*. Note that both the intrinsic accuracy and the limiting magnitude obtained with ALLFRAME are better than for ALLSTAR. Bottom panel: same as the top panel but the ALLSTAR reduction refers to the median image obtained using all the V-band images. The objects located at the bottom edge of the chip present larger intrinsic errors, since they have only been detected in a few images.

ALLFRAME presents at fixed magnitude a smaller intrinsic scatter when compared with ALLSTAR. As a matter of fact, σ_V, at $V \approx 23.5$, increases from ≈ 0.025 to ≈ 0.055. Moreover, the photometry performed with ALLFRAME is approximately one magnitude deeper than that one performed with ALLSTAR. In fact, the limiting magnitude, at $\sigma_V \approx 0.07$, decreases from $V \approx 23.8$, to 24,8, respectively. In this context it is worth mentioning that, the quoted tests were performed on V-band images for which we individually estimated the PSF. Therefore the difference in the photometric accuracy as well as in the limiting magnitude is due to different PSF-fitting algorithms.

As a further independent test, we derived the median V-band image using all the individual frames and then we performed the photometry on this image using ALLSTAR. This approach was adopted by Castellani M. et al. (2003) (these proceedings) to perform the photometry on

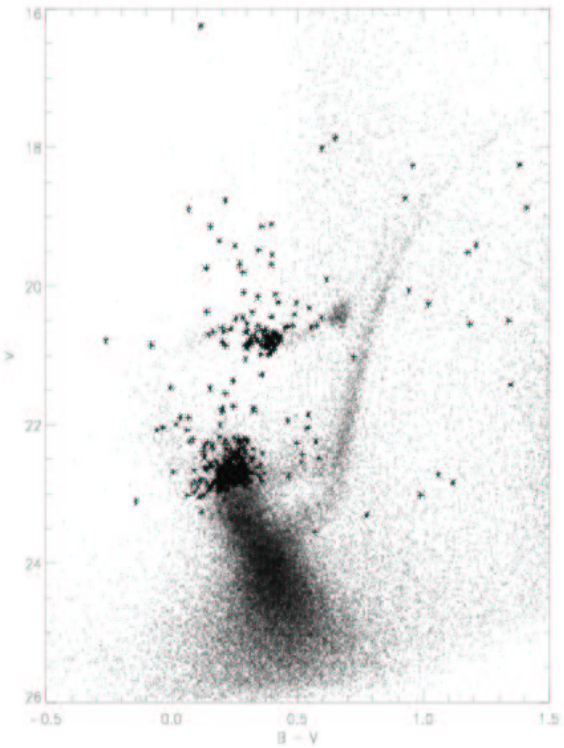

Fig. 3. Same as Figure 1, but stars mark candidate variable stars across the CMD.

the 2.2m dataset. The bottom panel of Fig. 2, shows the comparison between the two different strategies. Note that the intrinsic errors referred to the median image (ALLSTAR) were artificially shifted by one magnitude to avoid the crowding.

Data plotted in this figure show that the limiting magnitudes of the two different strategies are, as expected, quite similar. However, the comparison between the intrinsic accuracy given by ALLFRAME and by ALLSTAR discloses that the former one is better over the entire magnitude range.

3.1. Candidate variable stars

One of the main aims of this work is to detect stellar variability from the tip of the Red Giant Branch down to the MS Turn-Off. The search was performed using a variability index, similar to that introduced by Welch & Stetson (1993). This index is based on the dispersion of individual measurements around its mean value. The sum of the residuals around the mean magnitude weighted for the individual photometric error gives an estimate of the scatter, and in turn the variability of the source. We calculated this variability index for both B, V bands and we only selected the stars with $index > 2$ in both bands. We ended up with a sample of $\simeq 400$ stars (see Fig. 3). This sample includes RR Lyrae, Anomalous Cepheids, long-period variables close to the TRGB, and a sizable sample of δ Scuti stars.

4. Conclusions

We presented the results of a photometric investigation on the Carina dSph. Current photometry is based on data collected un-

der good seeing conditions with Mosaic Camera available at the 4m CTIO Blanco telescope. The new (V,B-V) CMD presents an interesting feature concerning the possible occurrence of extra-tidal stars.
We performed several experiments concerning the reduction strategy to perform the photometry. We found that ALLFRAME simultaneously executed over the entire set of images provides a better intrinsic accuracy and a deeper limiting magnitude when compared with ALLSTAR executed on individual images. The ALLFRAME intrinsic accuracy also shows a smaller dispersion when compared with the accuracy of the ALLSTAR photometry performed on the median image. This finding seems very promising in view of the systematic search of periodic and aperiodic variables in this stellar system.

Acknowledgements. Part of this work was supported by the Italian MIUR through the grant COFIN-2002028935 assigned to the project *Stellar populations in the Local Group Galaxies*

References

Castellani M. et al. 2003, MSAIt 74, 874
Dall'Ora M. et al. 2003, AJ, 126, 197
Harbeck, D., et al. 2001, AJ, 122, 3092
Monelli, M., et al. 2003, AJ, 126, 218
Kuhn, J. R. at al. 1996, ApJ, 469, 93
Johnston, K. V. at al. 1999, MNRAS, 302, 771
Kleyna et al., 2001, ApJ, 563, 115
Majewski et al., 2001, AJ, 119, 760
Mateo M. et al. 1998, AJ, 115, 1856
Mateo M. 1998, ARA&A,
Mighell, K. J. 1997, AJ, 114, 1458
Moore, B. et al. P. 1999, ApJ, 524, L19
Saha et al., 1986, AJ, 92, 302
Smecker-Hane T.A., Stetson P.B., Hesser J.E., Lehnert M.D. 1994, AJ, 108, 507
Stetson P.B. 1987, 99, 191
Stetson P.B. 1994, 106, 250
Stetson P.B. et al. 1998, PASP, 110, 533
Tolstoy et al. 2003, AJ, 125, 707
Valdes F. 1997, in ADASS VI, ed G. Hunt & H.E. Payne, (San Francisco: ASP), 455
Welch, D. L. & Stetson, P. B. 1993, AJ, 105, 1813